Jurnal Kejuruteraan 34(4) 2022: 605-615
https://doi.org/10.17576/jkukm-2022-34(4)-09



# Numerical Study of Hybrid Through Plate Connections to CFST Columns

Moussa Twizere* & Kıvanc Taşkin

*Department of Civil Engineering, Eskisehir Technical University, Turkey*

**Corresponding author: moussatwizere@eskisehir.edu.tr*

*Received 14 July 2021, Received in revised form 24 September 2021*
*Accepted 24 October 2021, Available online 30 July 2022*

ABSTRACT

*The use of concrete-filled steel tube (CFST) columns is highly encouraged nowadays in modern multistory structures. The major reason is the extensive resistance offered by the hollow steel column to high compression. Nevertheless, further studies and data are desirable to exhaustively characterize these members and their connections to other members, such as beams. This paper investigated the behavior of concrete-filled columns connected to I-beams by through plates. Three simple types of plate connections (easy to assemble and construct) were proposed and evaluated. The behavior of these connections was examined under static loading by using advanced finite element based software (ABAQUS). The modeling techniques used in this study were validated by comparing the numerical results of a through plate connection model with the results of two relevant experimental studies. The proposed connections were classified as semi-rigid connections according to Eurocode-3. These connections were able to move the plastic hinge away from the column panel zone. The maximum plastic rotations of all connection types were greater than 40 mrad. The failure mode, and moment-rotation curves of the concrete-filled column to steel beam connections were discussed based on numerical results. The influence of through plate material and through plate thickness were evaluated via a parametrical study.*

*Keywords: Numerical study; concrete filled column; I-beam; through plate; ABAQUS*

## INTRODUCTION

Nowadays concrete-filled steel tubular (CFST) columns are becoming more popular in high-rise buildings, particularly when the seismic loads are significant, because of their advantages, for example high load carrying capacity and ductility. In recent years the performance of concrete-filled column-beam connection has caught research considerations (Sheet et al. 2013; Erfani et al. 2016; Liu et al. 2021; Ding et al. 2021).

CFST column connection is one of the most important and challenging components of a CFST structural system. It plays a role in structural resilience during an earthquake. Research on several forms of CFST column-beam connection has been conducted, and new hybrid connections have also been suggested (Erfani et al. 2016; Ataei et al. 2016; Mou & Bai, 2018; Jiang & Chen, 2019; Zhang et al. 2020). A simple connection would be that the steel beam is connected directly to the steel tube skin for quick connections (Dunberry et al. 1987; Beena et al. 2017). Nevertheless, Alostaz & Schneider (1996) have shown that in moment resisting frames, the welding of the beam directly to the steel tube should not be used. Serious distortions of the tube wall can prevent the creation of the beam's plastic bending ability and cause very large stresses and strains on the flange weld and tube wall. Kosteski & Packer (2003) introduced a plate connection in which the plate passed through both walls of the hollow structural steel (HSS) member first and was then welded to the slotted tube. Voth & Jeffrey (2012) conducted a comparison study between the conventional (branch) plate - to - Circular hollow section (CHS) connections and "passing through" connections against transverse tensile and compressive forces with experimental as well as numerical investigations. Hoang et al. (2014) studied a through plate-to-CHS column connection where a through vertical plate was used to support the primary beams. Two horizontal plates, one at each side of the CHS, were welded to the upper side of the through-plate to facilitate the connection. Jiang & Chen (2019) proposed an innovative connection known as double-through plate connection, in which two plates pass through a slotted square column with the concrete infill, this connection was capable of limiting the plastic hinge in the panel zone. Das et al (2020) assess the characterization of trough plate connection of I-beam to hollow section column. The authors found that the design equation for chord plasticization against tensile and compressive forces of a traditional (branch) plate - to - rectangular hollow section (RHS) connection could be doubled for through plate-to-RHS connection. In concrete-filled stainless steel tubular columns, through plate connections were proven to be reliable for load transfer (Hassan et al. 2020). The findings indicated that combining full-through and half-through plates for connecting beams to CFSST columns is acceptable. Brahimi et al. (2021) introduced an innovative through-gusset plate connection. The proposed connection's cyclic behavior was evaluated via experimental study.

The results showed that through-gusset plate connection increased the strength of square-HSS and circular-HSS specimens. The steel beam-to-encased column composite connection was proposed by Azad et al. (2021). A vertical plate passed through the column and was linked to the steel beams as the connector. The recommended connection was able to achieve a story drift of 4%. When the full composite action of a steel-concrete composite beam is produced, the transferable bending capacity of the beam cross section increases.

It may be seen from the discussion above, that there is a need for CFST column to steel beam connections that are practical, easy to assemble, and provide good performance where the region of yielding is moved away from the panel zone. The present paper numerically investigated the performance of three proposed through plate connections. Three specimens were evaluated under static loading. The relevant numerical results were shown in detail. Based on the verified models, the influence of material and thickness of through plates on the connection response were analyzed. And finally, the behaviors of the connection were summarized.

## PROPOSED CONNECTIONS

In this work, as illustrated in Figure 1, three different configurations of through plate connections denoted TP-1, TP-2 and TP-3 were evaluated. For these connections, I-beam was connected to a box column by horizontal or vertical plates. The box column was filled with concrete. The connection of the beam to the plate was made by high-

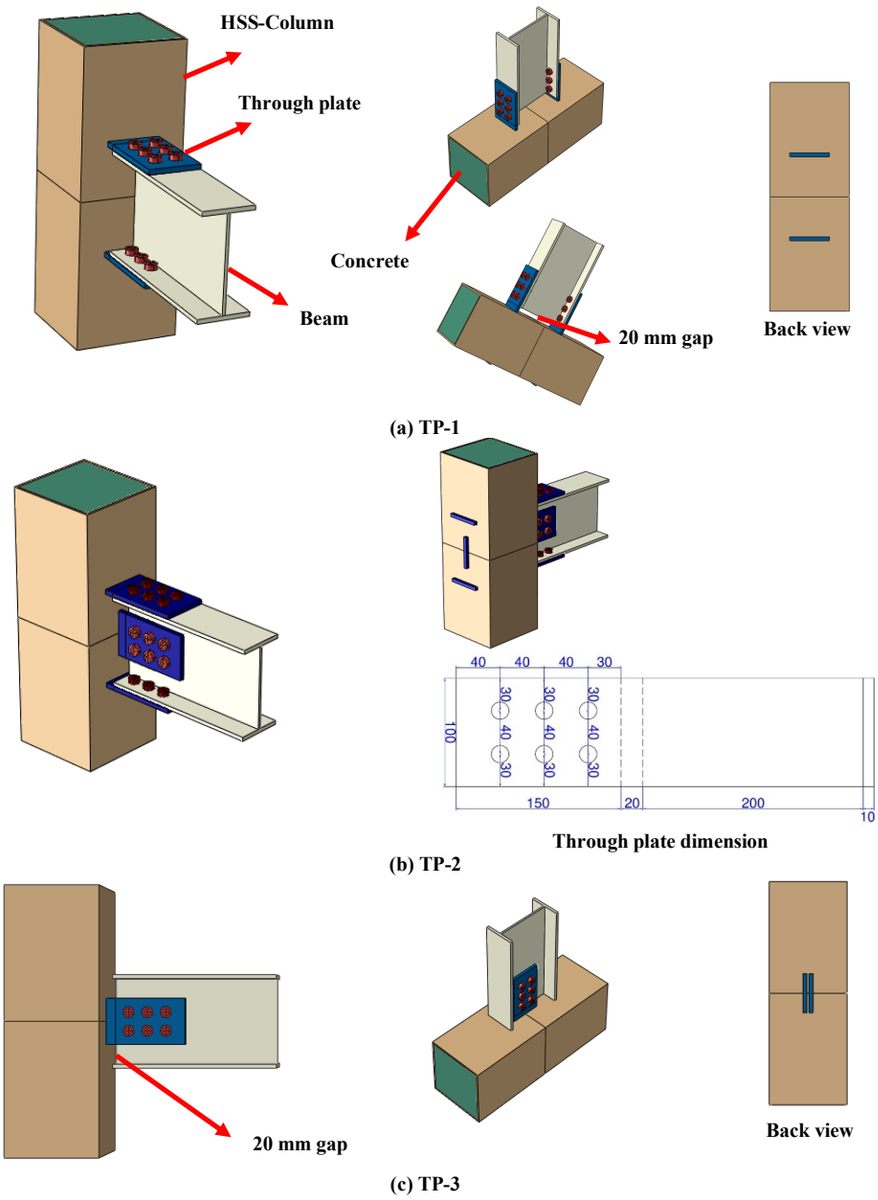


FIGURE 1. Proposed hybrid through plate connections

strength bolts. The beam was connected to HSS column with two horizontal through plates for the TP-1 connection (Figure 1(a)). For TP-2 the connection was reinforced by a vertical plate in the web (Figure 1(b)). While, for the TP-3 model, I-beam was connected to the column through two vertical plates in the web (Figure 1(c)). The plate used for all three models had the same geometrical and material properties. The gap between beam and column was considered to be 20 mm. The plates were designed to be easily assembled at the construction site. Column, beam, and bolts used for all specimens were designed as HSS of 200x200x5, IPE-200, and M16 respectively. The length of the beam was 1400 mm while the height of the column was 2300 mm. The thickness of the plate considered was 10 mm. The material properties used in this study can be found in Table 1. The concrete had 25 MPa of compressive strength.

TABLE 1. Material properties (Jiang& Chen 2019)

| Member | Yield Stress (MPa) | Ultimate stress (MPa) | Young's modulus (GPa) | Elongation at fracture (%) |
|---|---|---|---|---|
| Column | 341.8 | 501.4 | 211.3 | 26.9 |
| Beam | 331.1 | 472.8 | 208.2 | 25.4 |
| Plate | 241.4 | 383.1 | 213.5 | 27.8 |
| Bolt | 650 | 900 | 210 | 25 |

## NUMERICAL ANALYSIS

### GENERAL

In recent years, finite element-based software had been popular in beam-column connection modeling. The two most popular software are ABAQUS and ANSYS. These software are capable of predicting the behavior of simple or complex connections (Pirmoz et al. 2016; Nzabonimpa et al. 2018). In this work, numerical analysis was performed using ABAQUS. In this study, a finite element model of through plate connection was developed. Geometrical and material nonlinearities were considered. Finite element (FE) accuracy depends on the materials model, mesh types and size, boundary conditions, and contact elements.

### CONCRETE MODEL

Many experimental studies have been conducted to examine the behavior of concrete under uniaxial compression. Among numerous studies, Kent & Park (1975) established a numerical expression for the unconfined and confined stress-strain relationship model. In this study, Kent and Park confined concrete model was adopted. Figure 2 shows the confined model of 25 MPa concrete, where the ascending branch AB and descending branch (BC) were calculated by using Equations (1) to (3).

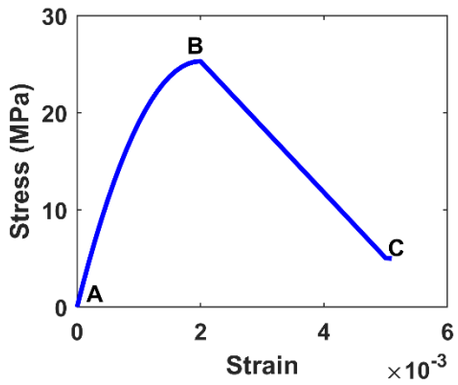


FIGURE 2. Confined concrete

For region AB: $\varepsilon_c \leq 0.002$

$$fc = f'_c[\frac{2\varepsilon_c}{0.002} - (\frac{\varepsilon_c}{0.002})^2] \quad (1)$$

For region BC: $\varepsilon_c \leq 0.002 \leq \varepsilon_{20c}$

$$f_c = f'_c[1 - z(\varepsilon_c - \varepsilon_{co}] \quad (2)$$

In which,

$$z = \frac{0.5}{\varepsilon_{50u} - \varepsilon_{co}}$$

$$\varepsilon_{50u} = \frac{3+0.29f'_c}{145f'_c-1000} \quad (f'_c \text{ in MPa}) \quad (3)$$

Where;

- fc : Longitudinal stress in concrete
- $\varepsilon_c$ : Longitudinal strain in concrete
- $f'_c$ : Concrete compressive cylinder strength
- $\varepsilon_{co}$ : Strain at maximum stress
- z : Slope of the descending branch of stress-strain curve
- $\varepsilon_{50u}$ : Strain corresponding to the stress equivalent to 50% of the maximum concrete strength of unconfined concrete
- $\varepsilon_{20c}$ : Strain corresponding to the stress equivalent to 20% of the maximum concrete strength of unconfined concrete

To predict the behavior of concrete material, ABAQUS offers crack models: a concrete damage plasticity model, a smacked crack concrete model, and a brittle concrete model. Among those, concrete damage plasticity is likely to represent the behavior of the concrete, in both compression and tension using damage parameters. The damage

parameters are dilation angle, eccentricity, Kc (the ratio of the second stress invariant on the tensile meridian to that on the compressive meridian), fb0/fc0 (ratio of initial equibiaxial compressive yield stress to initial compressive stress), and the viscosity parameters (ABAQUS, 2014). Dilation angles define the direction of the plastic strain. Malm (2006) conducted numerical and experimental investigations using dilation angles between 10° and 56.3° as shown in Figure 3. The author suggested that the dilation angles between 30° and 40° provided the best fit for concrete. The damage parameters of concrete are shown in Table. 2.

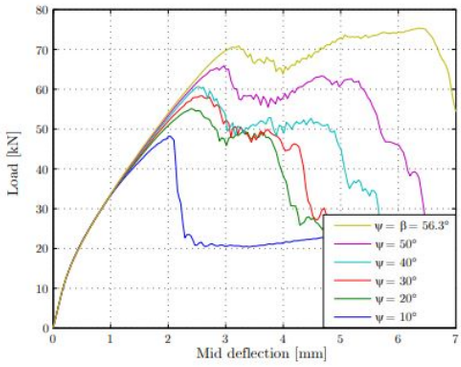


FIGURE 3. Influence of dilation angle in concrete damage plasticity model (Malm, 2006)

TABLE 2. Damage parameters (Zhou et al. 2019)

| Dilation Angle | Eccentricity | fb0/fc0 | K | Viscosity parameter |
|---|---|---|---|---|
| 40 | 0.1 | 1.225 | 0.66 | 0.001 |

## STEEL MODEL

An elastic-plastic model, considering Von Mises yielding criteria and isotropic strain hardening, was used to describe the constitutive behavior of steel. ABAQUS is expected to take true stress and true strain. Equations (4) and (5) were used to convert the normal stress and nominal strain to true stress and true strain. Figure 4 shows the steel material modeling in ABAQUS where nominal stress and strain were converted into true stress and true strain.

$$\sigma_{true} = \sigma_{nominal}(1 + \varepsilon_{nominal}) \quad (4)$$

$$\varepsilon_{true} = ln(1 + \varepsilon_{nominal}) \quad (5)$$

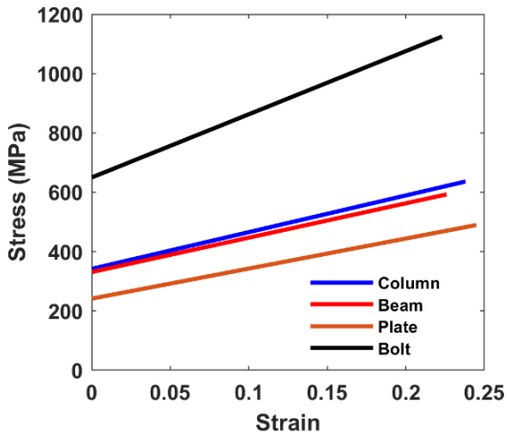


FIGURE 4. Steel material properties modeling in ABAQUS

## Mesh

For the analyses, a reduced integration element (C3D8R) meshing was adopted. The element stiffness matrix was established using a lower-order integration element. The use of a reduced integration element was considered in order to reduce the computational time of the FE models. In order to have an appropriate element shape, the structured meshing technique was used. The mesh sensitivity also was conducted, to find the appropriate size of mesh. The fine mesh size was used near the connection, while the dimension became coarser as one moved away from the panel zone.

## MODELING OF CONTACT ELEMENTS

ABAQUS supports surface-to-surface and node-to-node contact. Surface-to-surface contact was used instead of node-to-node contact to efficiently resolve the behavior of element contact. To prevent possible termination due to penetrations, master and slave surfaces must be clearly defined. Although the master surface node can penetrate the slave surface, the slave surface node cannot penetrate master surface. The master surface must be stiffer than the slave surface to accomplish this (Nzabonimpa et al. 2018). If two elements have the same material properties, the coarse mesh surface is the master surface. To connect the plates to the concrete, the embedded constraint was used. The host and embedded regions were made of concrete and plate respectively.

## BOUNDARY AND LOADING CONDITIONS

Columns were pinned at the top and the bottom, as shown in Figure 5. To model the pinned support, two rigid body were connected at both ends of the column. In order to apply load and eliminate stress concentration at the loading area, a rigid body was connected to the end of the beam. Also, lateral support was provided to restrict bending in a direction other than the loading direction (Figure 5).

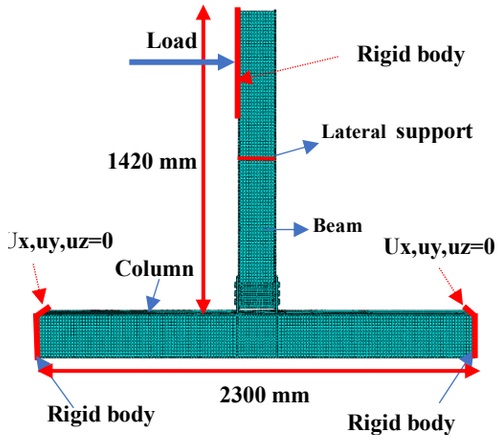


FIGURE 5. Connection model setup

The connection plastic rotation equal to 40 mrad is commonly used as benchmark to judge the seismic effectiveness of connections (AISC 341-16 (2016)). However, the plastic rotation greater than 40 mrad is desirable. In this study, the displacement loading protocol was adopted. The rotation in the connection was increased in small increments. The nonlinear effects of large displacement were also taken into account. A damping factor of 0.0002 was introduced to solve the convergence problem (Nzabonimpa et al. 2018).

## FINITE ELEMENT MODEL VALIDATION

To verify the proposed FE model, the experimental study of a trough plate connection conducted by (Jiang & Chen, 2019) was used. Hollow square steel beam was connected to a concrete-filled steel tube by a double through plate connection. Two specimens of square column were designed as 250×250×5 mm (denoted as SJ1) and 250×250×8 mm (denoted as SJ2). The cross-section of all steel HSS beams was 300×150×8×10 mm, where the digits respectively refer to section height, section width, web thickness, and flange thickness. The length of the beam was 1400 mm while the height of the column was 2300 mm. The plate thickness was 10 mm. All bolts used in the test were Grade 10.9 M24. While all bolt holes on beam webs were 26 mm in diameter and have an oval shape. The steel material properties are shown in Table 1. The concrete had 25.3 MPa of compressive strength.

Figure 6 (a) and Figure 6 (b) show the applied load and embedded constraint respectively. The embedded

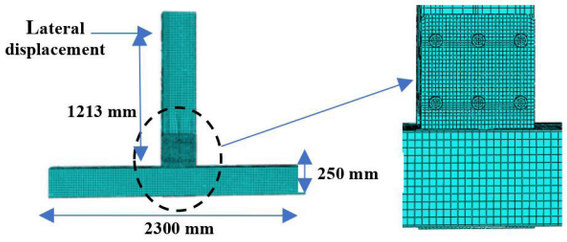


(a) Load displacement control

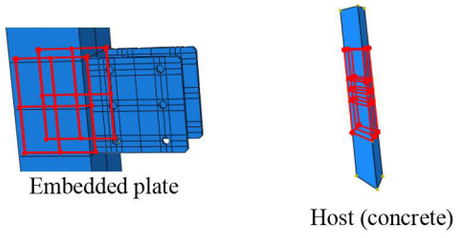


(b) Embedded constraint

| Interaction type | Master surface | Slave surface |
|---|---|---|
| Int-1 | Right bolt | Right Plate and hole |
| Int-2 | Left bolt | Left Plate and hole |
| Int-3 | Right beam | Right plate |
| Int-4 | Left beam | Left plate |

(c) Surface to surface interaction

| Constraint type | Master surface | Slave surface |
|---|---|---|
| Rigid- top | Rigid-1 | Beam |
| Rigid –bot | Rigid-2 | Top of column |
| Rigid- beam | Rigid -3 | Bot of column |
| Concrete to column | HSS | concrete |

(d) Tie constraint

FIGURE 6. Mesh and contact elements

constraint represents the contact between through plate and concrete. Four interactions were assigned to represent the contact formulation for the executed FE models as depicted in Figure 6 (c). Also, four tie constraints were assigned to connect the rigid body at the top of the column, the bottom of the column, and at the end of the beam. Filled concrete was also tied to the HSS as shown in Figure 6 (d).

To verify the proposed FE model with experimental study, the moment rotation curve and failure mode were examined. The bending moment and rotation were obtained as indicated in Equations (6) and (7) respectively.

$$M = P \times L \tag{6}$$

$$\theta = \Delta / L \tag{7}$$

Figure 7 (a) illustrates the comparisons of moment-rotation curves for SJ1 (experiment) and the proposed FE model. While, Figure 7(a) illustrates the comparisons of moment-rotation curves for SJ1 (experiment) and the proposed FE model. While, Figure 7(b) represents the comparison of moment-rotation curves for SJ2 (experiment) and the proposed FE model. The difference in maximum moment was 1.9 % for SJ1 (experiment) compared with the FE-Model. The difference in maximum moment was 5.4 % for SJ2 (experiment) compared with the FE model. It can be concluded that the moment rotation curves for experimental studies and the FE-Model accurately predict the moment of through plate connection.

The failure mode of experimental study and the FE-Model were compared (Figure 8). In ABAQUS, the equivalent plastic strain (PEEQ) describes the accumulation of plastic strain in materials, and this coefficient is generally used to analyze plasticity development. When the material enters the yielding state, the PEEQ value will be greater than zero and will increase as the plastic deformation increases. Therefore, the plastic zone conditions in the connection can be distinguished based on the PEEQ contours diagram. In the experimental study (SJ1), the failure was governed by the fracture of the through plate (Figure 8(a)). As it can be seen in Figure 8(b), the maximum concentration of PEEQ values was at the same level as the plate fracture level in the experiment.

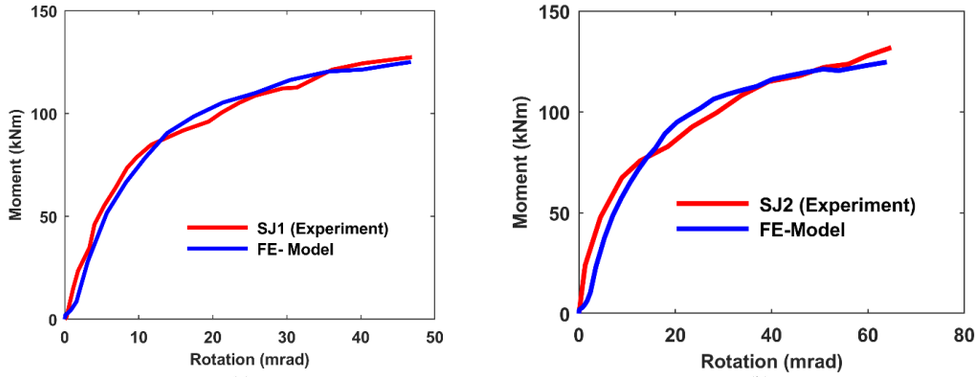


FIGURE 7. Moment rotation curve comparison; a) SJ1 with FE-Model, b) SJ2 with FE-Model

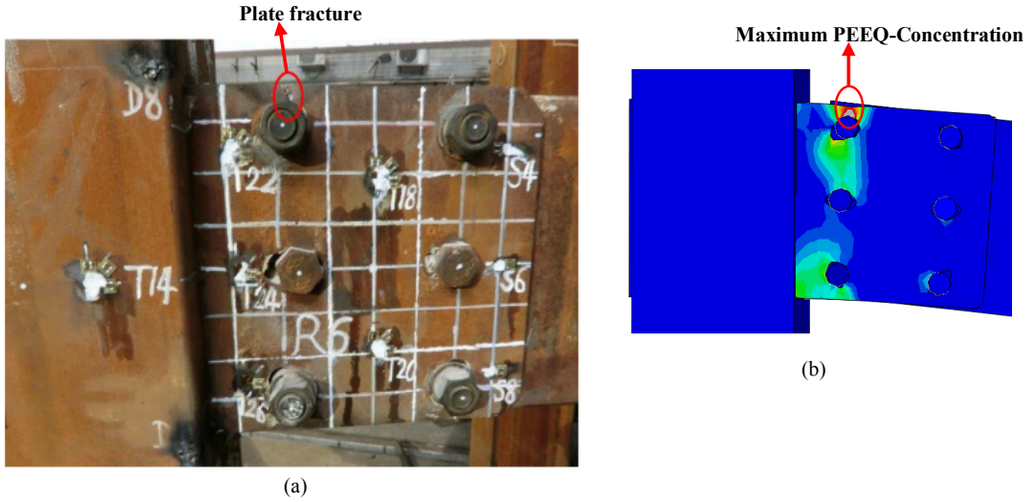


FIGURE 8. The failure mode; a) Experiment, b) FE-Model

## ANALYSIS RESULTS

### MOMENT ROTATION

The beam-column connection must transfer the bending moment. To study the bending moment transfer of the proposed connections, the moment rotation curves were examined (Figure 9). The beam was connected to the column via; horizontal plates (TP-1), vertical plates (TP-3), and a combination of horizontal and vertical plates (TP-2). The TP-1 connection exhibited a bending moment capacity of 83.6 % greater than TP-3. This is due to the fact that the web of the beam does not have as much capacity to resist bending moments as the beam's flange.

The moment-rotation relationship shows that the capacity of the connection increases when both beam flange and web are connected to the column as presented in Figure 9 (refer to TP-2 Model). The TP-2 connection was able to exhibit a 22.5% moment greater than the TP-1 connection. TP-2 connection exhibited a moment capacity greater than TP-1, because the vertical plate available in the TP-2 connection was able to limit the local buckling that occurred in the beam for the TP-1 connection.

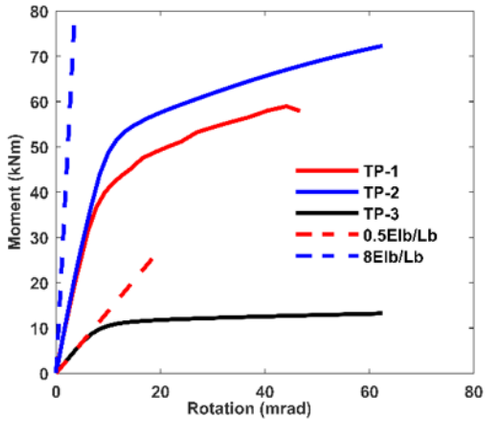


FIGURE 9. Moment rotation Relationship

## JOINTS CLASSIFICATION

The proposed connections exhibited different initial stiffness, as can be seen in Figure 9. The initial stiffness represents the angle between moment and rotation in the elastic part. The TP-1 connection offered 6% less initial stiffness than TP-2. This is due to the presence of a vertical plate in the TP-2 connection. Connecting beam to column trough flange (refer to TP-1) exhibited greater initial stiffness than connecting it with through web (refer to TP-3). The initial stiffness of TP-1 was 75% greater than TP-3. The Eurocode (EN 1993-1-8) classifies the joint by stiffness. The joint can be classified as rigid, semi-rigid or nominal pinned, referring to the initial stiffness. The joint is rigid, if $S_{ij} > k_b EI_b/L_b$; where $k_b$=8 for non-sway frames. The joint is nominally pinned, if $S_{ij} < 0.5EI_b/L_b$; Otherwise, it is semi-rigid. Here, $EI_b$ and $L_b$ is the flexural stiffness and the length of steel beam respectively. $S_{ij}$ is the initial rotational stiffness of the connection. The boundary of the proposed connections classifications are shown in Figure 9. Accordingly, TP-1, and TP2 were classified as semi rigid, while TP-3 as nominal pinned connection.

### FAILURE MODE OF PROPOSED CONNECTIONS

The failure of the connection was mainly caused by the failure of the plate, as the distribution of plastic strain for TP-1, TP-2, and TP-3 is shown in Figure 10 to Figure 12.

The maximum equivalent plastic strain was found to be at the holes of the first bolt row for all connections. For the TP-1 connection, local buckling of the beam's web and buckling of the bottom flange occurred. The addition of the vertical plate (refer to TP-2), avoided the creation of local buckling in the beam. Also, it prevented the bottom plate from buckling as in the TP-1 connection. All of these connections were able to prevent the yielding of the column.

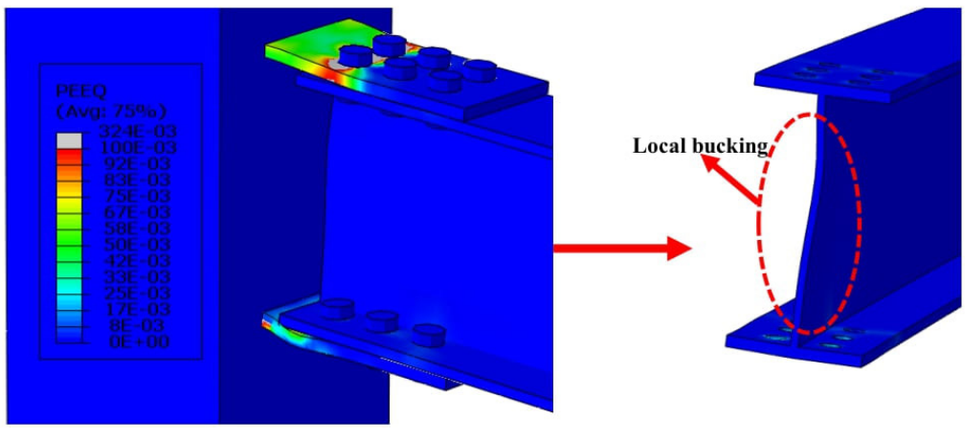


FIGURE 10. Equivalent plastic strain for TP-1

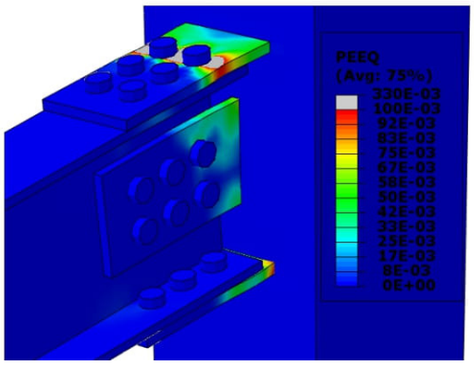


FIGURE 11. Equivalent plastic strain for TP-2

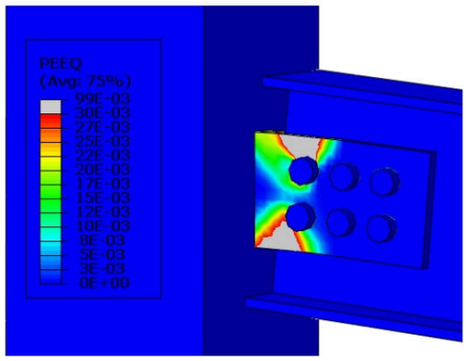


FIGURE 12. Equivalent plastic strain for TP-3

PARAMETRICAL STUDY

PLATE THICKNESS

The influence of the thickness of the plate on the TP-1 connection was evaluated. The material and geometry properties were kept constant, only the plate thickness changed. Figure 13 presents the moment rotation curves of TP-1-X. Where, X represents the thickness of the plate. The plate thickness varies from 5 to 17 mm. The moment capacity of the connection increases with the plate thickness (Figure 13). This is due to the increase of the bending capacity of the plate. As the thickness of the plate increases, the bending capacity of the plate also increases, as shown in Table 3. The bending capacity of the plate or beam can be calculated by using Equation (8). Where; fy, Z represent yield strength and plastic modulus, respectively.

$$Mp = \mathrm{fy} * \mathrm{Z} \tag{8}$$

The thickness of the plate also has an effect on the rotation capacity. The ductility of the plate reduces as thickness increases (Wang et al. 2013). TP-1-5 connection rotated at 45.3 mrad, while TP-1-17 connection rotated at 34.6 mrad. The rotation of TP-1-17 was smaller than other connections (Figure 13).

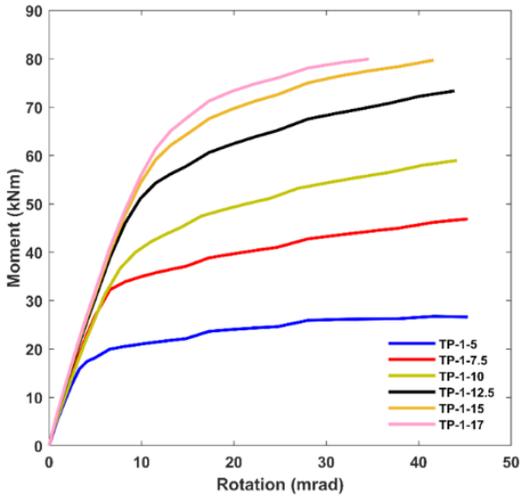


FIGURE 13. Moment rotation of TP-1 with different plate thickness

For the thickness of the plate ranging from 5 to 10 mm, the failure was found to be governed by the plate bucking. Figure 14 (a) shows the failure mode of a connection with a 5 mm thickness (TP-1-5). No local buckling in the beam web was found in this connection. Also, excessive buckling was found in the top and bottom plates. However, as the thickness of the plate increased, the connection tends to develop local buckling in the beam's web. For the connection with a thickness of plate equal to 12.5 mm or greater, the failure was governed by the plate buckling and local buckling of the beam's web. Figure 14 (b) shows the failure mode of TP-1-15. The formation of local buckling in the beam depend on the thickness ratio between beam's flanges plus plate to beam's web. As this ratio increased, the probability of formation of local buckling increased.

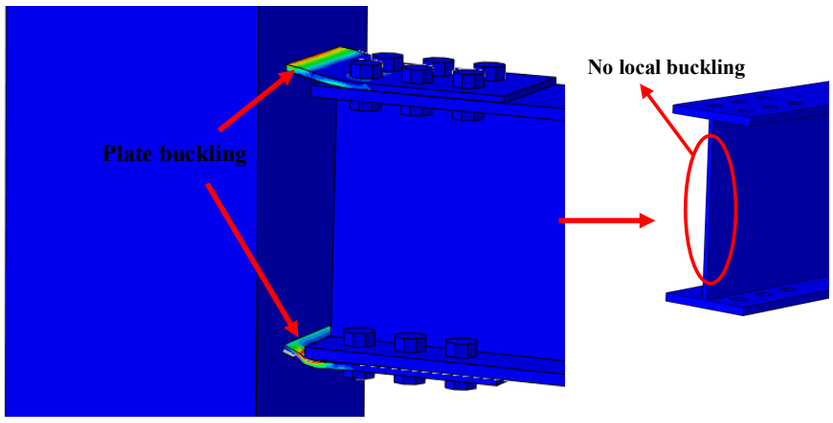


(a)

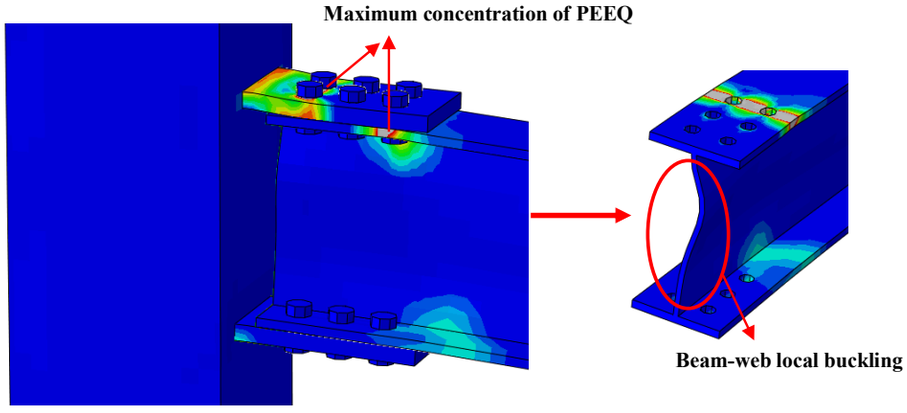


(b)

FIGURE 14. The Failure mode of ; a) TP-1-5 b) TP-1-15

## PLATE MATERIALS

To evaluate the influence of material properties of the plate on the connection behavior, the plate yield and ultimate stresses were changed. The yield and ultimate stresses of the beam were multiplied by a coefficient ranging from 0.8 to 1.5 and then assigned to the plate. This choice was made so that the material would be in the range given by Eurocode -3 material classes (S235, S275, S355, and S450). Other properties were kept constant. The ultimate moment of the connections increases with the increase of plate yield strength as shown in Table 4. This is due to the increase of the plastic moment (bending capacity) of the plate (Table 3). The first yield point for the plate and beam was found to be in the vicinity of the hole. It was found that the first yield point is related to the bending capacity of the plate and beam. As the plate yield strength increased, the bending capacity of the plate increased.

Table 3 presents the percentage to the yield point for plate, beam, and column. Its shows that when the plastic moment of the plate ($Mp_p$) was less than 1.4 times the plastic moment of the beam's flange ($Mp_b$), the first yield point occurred in the plate. However, for the plastic moment of the plate between 1.4 to 2 times the plastic moment of the beam 'flange, the first yield points was created in the plate and beam at the same time. When the ratio $Mp_p/Mp_b$ was greater than 2, the first yield point was created in the beam. The change in material did not produce any yield point in the column.

TABLE 3. Percentage to the yield point

| Model | Plate Thickness (mm) | $Mp_p/Mp_b$ | % to Yield point | | |
|---|---|---|---|---|---|
| | | | Plate | Beam | Column |
| TP-1-5 | 5 | 0.2 | 100 | 36.2 | 11.9 |
| TP-1-7.5 | 7.5 | 0.5 | 100 | 40.5 | 11.3 |
| TP-1-10 | 10 | 0.9 | 100 | 75.2 | 8.6 |
| TP-1-12.5 | 12.5 | 1.4 | 100 | 100 | 16.1 |
| TP-1-15 | 15 | 2.0 | 100 | 100 | 20.6 |
| TP-1-17 | 17 | 2.6 | 82.2 | 100 | 25.4 |
| 0.7fy-0.7fu | 10 | 1.0 | 100 | 65.1 | 7.0 |
| 0.8fy-0.8fu | 10 | 1.1 | 100 | 90.5 | 11.2 |
| 0.9fy-0.9fu | 10 | 1.2 | 100 | 90.7 | 11.2 |
| fy-fu | 10 | 1.4 | 100 | 100 | 15.7 |
| 1.1fy-1.1fu | 10 | 1.5 | 100 | 100 | 15.7 |
| 1.3fy-1.3fu | 10 | 1.8 | 100 | 100 | 20.4 |
| 1.5fy-1.5fu | 10 | 2.1 | 79.9 | 100 | 15.7 |

Where: $Mp_p$ is bending capacity of the plate, $Mp_b$ is the bending capacity of beam's flange

TABLE 4. Stiffness with different plate materials

| Plate Material | | Initial Stiffness | Ultimate Moment |
|---|---|---|---|
| Yield strength | Ultimate strength | (kNm/rad) | (kNm) |
| 0.7fy | 0.7fu | 4370.83 | 55.21 |
| 0.8fy | 0.8fu | 4644.00 | 61.69 |
| 0.9fy | 0.9fu | 3635.71 | 66.23 |
| fy | fu | 3500.00 | 69 |
| 1.1fy | 1.1fy | 3739.52 | 72 |
| 1.3fy | 1.3fu | 3868.47 | 74 |

## CONCLUSION

Connecting beam to concrete filled column is very challenging due to the formation of the hinge in the column panel zone. In this work, through plate connections capable of moving away the hinge from the column panel zone were proposed and analyzed. The following conclusions can be drawn based on the study in this paper:

(1) Finite element models can be used to predict the ultimate strength and rotation of through plate connections, with satisfactory accuracy. FE models can be presented as an alternative solution to high-cost experimental studies.

(2) The comparison of through plate connections shows that connecting only the beam's web to the column decreases the ultimate strength of the connection. However, the ductility of the connection increases.

(3) It was found that connecting the beam's flange to the concrete filled column gives more strength compared to connecting beam's web. The inclusion of a web stiffener increases the capacity of the connection.

(4) Increasing the thickness of the through plate increases the strength of the connection. However, the rotation capacity decreases.

(5) If the proposed connection is designed so that the beam yield, the ratio of plastic moment between through plate and beam's flange must be greater than 1.4.

(6) Through plate connections are easy to assemble and provide good performance. In these types of connections, the region of yielding is moved away from the column panel zone.

## ACKNOWLEDGEMENT

The authors would like to thank to Gujarat Technological University for supporting this research.

## DECLARATION OF COMPETING INTEREST

None

## REFERENCES

AISC Committee on Specification. 2016. *Seismic Provisions for Structural Steel Buildings*. Chicago, Illinois.

Alostaz, Y.M., & Schneider, S.P. 1996. Analytical behavior of connections to concrete-filled steel tubes. *Journal of Constructional Steel Research* 40(2): 95-127.

Ataei, A., Bradford, M.A., & Valipour, H.R. 2016. Finite element analysis of HSS semi-rigid composite joints with precast concrete slabs and demountable bolted shear connectors. *Finite Elements in Analysis and Design* 122: 16-38.

Azad, S., Mirghaderi, S. R., & Epackachi, S. 2021. Numerical investigation of steel and composite beam-to-encased composite column connection via a through-plate *Structures* 31: 14-28.

Beena, K., Naveen, K., & Shruti, S. 2017. Behaviour of bolted connections in concrete-filled steel tubular beam-column joints. *Steel and Composite Structures* 25(4):443-456.

Das, R., Kanyilmaz, A., Couchaux, M., Hoffmeister, B., & Degee, H. 2020. Characterization of moment resisting I-beam to circular hollow section column connections resorting to passing-through plates. *Engineering Structures* 210: 110356.

Dassault Systèmes Simulia Corp. 2016. *ABAQUS Analysis User's Manual 6.14-2*. Providence, RI, USA.

Ding, C., Bai, Y., Yang, K., & Zhang, J. 2021. Cyclic behaviour of prefabricated connections for steel beam to concrete filled steel tube column. *Journal of Constructional Steel Research* 176: 106422.

Dunberry, E., LeBlanc, D., & Redwood, R. G. 1987. Cross-section strength of concrete-filled HSS columns at simple beam connections. *Canadian Journal of Civil Engineering* 14(3): 408-417.

Ebrahimi, S., Mirghaderi, S. R., Zahrai, S. M., Najafi, A., & Otaghsaraie, S. M. S. 2021. Experimental study on brace to HSS column connection using through-gusset plate. *Engineering Structures* 234: 111948.

Erfani, S., Asnafi, A.A., & Goudarzi, A. 2016. Connection of I-beam to box-column by a short stub beam. *Journal of Constructional Steel Research* 127: 136-150.

Eurocode 3. 2005 *Design of Steel Structures Part 1-8: Design of Joints. EN 1993-1-8*. Brussels.

Hassan, M. K., Tao, Z., & Katwal, U. 2020. Behaviour of through plate connections to concrete-filled stainless steel columns. *Journal of Constructional Steel Research* 171: 106142.

Hoang, V.L., Demonceau, J.F., & Jaspart, J.P. 2014. Resistance of through-plate component in beam-to-column joints with circular hollow columns. *Journal of Constructional Steel Research* 92: 79-89.

Jiang, J., & Chen, S. 2019. Experimental and numerical study of double-through plate connections to CFST column. *Journal of Constructional Steel Research* 153: 385-394.

Kosteski, N., & Packer, J.A. 2003. Longitudinal plate and through plate-to-hollow structural section welded connections. *Journal of Structural Engineering* 129(4): 478-486.

Liu, H., Hao, J., Xue, Q., & Sun, X. 2021. Seismic performance of a wall-type concrete-filled steel tubular column with a double side-plate I-beam connection. *Thin-Walled Structures* 159: 107175.

Malm, R. 2006. Shear cracks in concrete structures subjected to in-plane stresses. PhD thesis, KTH Royal Institute of Technology, Stockholm, Sweden.

Mou, B., & Bai, Y. 2018. Experimental investigation on shear behavior of steel beam-to-CFST column connections with irregular panel zone. *Engineering Structures* 168: 487-504.

Nzabonimpa, J. D., & Hong, W. K. (2018). Use of artificial damping factors to enhance numerical stability for irregular joints. *Journal of Constructional Steel Research,* 148: 295-303.

Park, R., & Paulay, T. 1975. Reinforced concrete structures. John Wiley & Sons.

Pirmoz, A., Ahadi, P., & Farajkhah, V. 2016. Finite element analysis of extended stiffened end plate link-to-column connections. *Steel Construction* 9(1): 46-57.

Sheet, I.S., Gunasekaran, U., & MacRae, G.A. 2013. Experimental investigation of CFT column to steel beam connections under cyclic loading. *Journal of Constructional Steel Research* 86: 167-182.

Voth, A.P., & Packer, J.A. 2012. Branch plate-to-circular hollow structural section connections. II: X-type parametric numerical study and design. *Journal of structural engineering* 138(8): 1007-1018.

Wang, Y. Q., Liu, X. Y., Hu, Z. W., & Shi, Y. J. 2013. Experimental study on mechanical properties and fracture toughness of structural thick plate and its butt weld along thickness and at low temperatures. *Fatigue & fracture of engineering materials & structures* 36(12): 1258-1273.

Zhang, A.L., Zhang, H., Jiang, Z.Q., Li, C., & Liu, X.C. 2020. Low cycle reciprocating tests of earthquake-resilient prefabricated column-flange beam-column joints with different connection forms. *Journal of Constructional Steel Research* 164: 105771.

Zhou, Q.S., Fu, H.W., Ding, F.X., Liu, X.M., Yu, Y.J., Wang, L.P., Yu, Z.W., & Luo, L. 2019. Seismic behavior of a new through-core connection between concrete-filled steel tubular column and composite beam. *Journal of Constructional Steel Research* 155*:* 107-120.